

# Phase diagram and thermal properties of strong-interaction matter

Fei Gao,<sup>1</sup> Jing Chen,<sup>1</sup> Yu-Xin Liu,<sup>1,2,3,\*</sup> Si-Xue Qin,<sup>4</sup> Craig D. Roberts,<sup>4,†</sup> and Sebastian M. Schmidt<sup>5</sup>

<sup>1</sup>*Department of Physics and State Key Laboratory of Nuclear Physics and Technology, Peking University, Beijing 100871, China*

<sup>2</sup>*Collaborative Innovation Center of Quantum Matter, Beijing 100871, China*

<sup>3</sup>*Center for High Energy Physics, Peking University, Beijing 100871, China*

<sup>4</sup>*Division of Physics, Argonne National Laboratory, Argonne, IL 60439, USA*

<sup>5</sup>*Institute for Advanced Simulation, Forschungszentrum Jülich and JARA, D-52425 Jülich, Germany*

(Dated: 26 June 2015)

We introduce a novel procedure for computing the  $(\mu, T)$ -dependent pressure in continuum QCD; and therefrom obtain a complex phase diagram and predictions for thermal properties of the system, providing the in-medium behaviour of the trace anomaly, speed of sound, latent heat and heat capacity.

PACS numbers: 25.75.Nq, 11.10.Wx, 12.38.Lg, 21.65.Qr

*1:Introduction.*—Strong interactions in the Standard Model are described by quantum chromodynamics (QCD), which is supposed to describe a vast array of phenomena, from gluon and quark interactions at the highest energies achievable with the large hadron collider (LHC), through the structure of nuclei at long range, to the nature of nuclear material at the heart of a compact star. This last question initiated the quest to uncover the equation of state (EoS) for superdense nuclear matter, forty years ago [1]. The intervening years have seen remarkable activity, highlighted by completion of the relativistic heavy-ion collider (RHIC) [2] and discovery of a new state of matter, *viz.* a strongly-coupled quark-gluon plasma (sQGP) [3]. These efforts have delivered a sketch of the QCD EoS in the plane spanned by baryon chemical potential ( $\mu_B$ ) and temperature ( $T$ ) [4, 5].

In vacuum, *i.e.* in the neighbourhood  $\mu_B \simeq 0 \simeq T$ , QCD exists in a phase characterised by two emergent phenomena: confinement and dynamical chiral symmetry breaking (DCSB). Confinement is most simply defined empirically: those degrees-of-freedom used in defining the QCD Lagrangian – gluons and quarks – do not exist as asymptotic states, *i.e.* these partonic excitations do not propagate with integrity over length-scales that exceed some modest fraction of the proton’s radius ( $r_p \approx 0.9$  fm). The forces responsible for confinement appear to generate more than 98% of the mass of visible matter [6]. This phenomenon is known as DCSB. It is an essentially quantum field theoretical effect, which is expressed and explained via the appearance of momentum-dependent mass-functions for quarks [7–10] and gluons [11–15] even in the absence of any Higgs-like mechanism.

On the other hand, in medium, *i.e.* as  $\mu_B$  and/or  $T$  are increased beyond certain critical values, the property of asymptotic freedom [16–18] suggests that QCD undergoes phase transitions. In the new phases, chiral symmetry is restored and/or gluons and quarks are deconfined. Indeed, the possibility that the transitions are related and coincident in the  $(\mu_B, T)$ -plane is much discussed.

The QCD EoS and related thermal properties are im-

portant for numerous reasons, many related to the nature and evolution of the early universe [19]. More prosaically, they are required as inputs to the hydrodynamic simulations which are necessary in order to connect basic theoretical predictions with experimental data obtained at RHIC and LHC. In this connection, the current sketches are not adequate: a better picture is needed in order to understand the data and hence the qualities of a sQGP.

The  $T \neq 0$  properties of QCD have been scrutinised via simulations of the lattice-regularised theory (lQCD). This is apparent, *e.g.* in Ref. [20], which also highlights the problems encountered in attempting to extend lattice methods to  $\mu_B \neq 0$  because of the ubiquitous fermion sign problem [21]. At this stage, a picture of the phase diagram in the entire  $(\mu_B, T)$ -plane requires other methods, so models continue to be employed widely. However, they are numerous in number and various in formulation, and too often provide conflicting predictions [20]. Herein, therefore, we analyse the thermal properties of QCD using methods of continuum quantum field theory; namely, the Dyson-Schwinger equations (DSEs) [22–26].

*2:Dressed-quark pressure.*—We focus on thermal properties associated with the matter sector of QCD and hence begin with the quark gap equation:

$$S(\vec{p}, \tilde{\omega}_n)^{-1} = i\vec{\gamma} \cdot \vec{p} + i\gamma_4 \tilde{\omega}_n + m + \Sigma(\vec{p}, \tilde{\omega}_n), \quad (1a)$$

$$\begin{aligned} \Sigma(\vec{p}, \tilde{\omega}_n) &= T \sum_{l=-\infty}^{\infty} \int \frac{d^3q}{(2\pi)^3} g^2 D_{\mu\nu}(\vec{p}-\vec{q}, \Omega_{nl}; T, \mu) \\ &\times \frac{\lambda^a}{2} \gamma_\mu S(\vec{q}, \tilde{\omega}_l) \frac{\lambda^a}{2} \Gamma_\nu(\vec{q}, \tilde{\omega}_l, \vec{p}, \tilde{\omega}_n), \end{aligned} \quad (1b)$$

where  $m$  is the current-quark bare-mass;  $\tilde{\omega}_n = \omega_n + i\mu$ ,  $\omega_n = (2n+1)\pi T$  is the quark Matsubara frequency and  $\mu$  is the quark chemical potential ( $\mu_B = 3\mu$ ),  $\Omega_{nl} = \omega_n - \omega_l$ ;  $D_{\mu\nu}$  is the dressed-gluon propagator; and  $\Gamma_\nu$  the dressed-quark-gluon vertex. (Regularisation and renormalisation are straightforward and detailed elsewhere [27–29]).

$$\begin{aligned} S(\vec{p}, \tilde{\omega}_n)^{-1} &= i\vec{\gamma} \cdot \vec{p} A(\vec{p}^2, \tilde{\omega}_n^2) \\ &+ i\gamma_4 \tilde{\omega}_n C(\vec{p}^2, \tilde{\omega}_n^2) + B(\vec{p}^2, \tilde{\omega}_n^2). \end{aligned} \quad (2)$$

The kernel of Eq. (1) is determined by the quark-gluon vertex and the gluon propagator. Regarding the former, we use  $\Gamma_\nu = \gamma_\nu$ , which defines rainbow-ladder (RL) truncation, *i.e.* the leading-order in the most widely used symmetry-preserving DSE approximation scheme [30, 31]. The RL truncation is accurate for properties of ground-state isospin-nonzero pseudoscalar- and vector-mesons, and the nucleon and  $\Delta$ -baryon [22–26]. It is appropriate here because whilst a certain class of vertex improvements can influence critical exponents associated with second order transitions, *viz.* those leading to inclusion of long-range colour-singlet correlations [32], no form available today alters the order of a transition or has a material impact on its location [33–35].

The gluon propagator in Eq. (1) has the general form

$$\frac{g^2}{8\pi^2} D_{\mu\nu}(\vec{k}, \Omega) = P_{\mu\nu}^T D_T(\vec{k}^2, \Omega^2) + P_{\mu\nu}^L D_L(\vec{k}^2, \Omega^2), \quad (3)$$

where  $P_{\mu\nu}^{T,L}$  are, respectively,  $\vec{k}$  transverse and longitudinal projection operators, and  $P_{\mu\nu}^T + P_{\mu\nu}^L = \delta_{\mu\nu} - k_\mu k_\nu / k^2$ ;  $D_T = \mathcal{D}(s_\Omega, 0)$ ,  $D_L = \mathcal{D}(s_\Omega, m_g^2)$ , where  $m_g^2 = (16/5)(T^2 + 6\mu^2/[5\pi^2])$  describes a gluon screening mass, the value of which is determined from leading-order perturbative QCD [36]; and  $(s_\Omega = \Omega^2 + \vec{k}^2 + m_g^2)$  [37]

$$\mathcal{D}(s_\Omega, m_g^2) = \frac{D}{\omega^4} e^{-s_\Omega/\omega^2} + \frac{\gamma_m \mathcal{F}(s_\Omega)}{\ln[\tau + (1 + s_\Omega/\Lambda_{\text{QCD}}^2)^2]}, \quad (4)$$

with  $z\mathcal{F}(z) = (1 - e^{-z/4\omega^2})$ ,  $\omega = 0.5 \text{ GeV}$ ,  $\tau = e^2 - 1$ ,  $\gamma_m = 12/25$ ,  $\Lambda_{\text{QCD}} = 0.234 \text{ GeV}$ .  $\mathcal{D}(s_\Omega, m_g^2)$  is shape-consistent with solutions of the in-vacuum gauge sector gap equations [15]; and with the mass-scale set via  $D\omega = (0.8 \text{ GeV})^3$  and a renormalisation-group-invariant current-quark mass  $\hat{m}_{u,d} = 6 \text{ MeV}$ , the solutions of Eq. (1) support a reliable in-vacuum description of ground-state hadrons in RL truncation [37].

The in-medium extension of the gap equation's kernel, Eq. (4), preserves agreement with QCD at large momenta. However, in assuming that  $D$  is  $(\mu, T)$ -independent it overlooks screening of the interaction's infrared strength. We remedy that by writing [33, 34]

$$D(T, \mu) = D \begin{cases} 1, & T < T_p, \\ \frac{a}{b(\mu) + \ln[\tilde{T}/\Lambda_{\text{QCD}}]}, & T \geq T_p, \end{cases} \quad (5)$$

where  $\tilde{T}^2 = T^2 + 6\mu^2/[5\pi^2]$  and  $T_p$  denotes the onset-scale for thermal screening. At  $\mu = 0$ , we set  $T_p = T_c$ , where  $T_c$  is the critical temperature for chiral symmetry restoration; then with  $a = 0.029$ ,  $b = 0.47$  one obtains a dressed-quark thermal mass  $m_T = 0.8T$  at  $T = 2T_c$ , in agreement with lQCD simulations [38]. Naturally,  $T_c = T_c(\mu)$ , in which case we set  $T_p(\mu) = T_c(\mu)$  at  $\mu \neq 0$  and ensure  $D(T_c(\mu), \mu) = D$  by evolving the value of  $b(\mu)$ .

In RL truncation and stationary phase approximation, the dressed-quark pressure is [39]:

$$P[S] = \frac{T}{V} \ln Z = -\frac{T}{V} \left( \text{Tr} \ln [TS] + \frac{1}{2} \text{Tr} [\Sigma S] \right), \quad (6)$$

where  $S$ ,  $\Sigma$  are determined from a solution to Eq. (1). At each  $(\mu, T)$ , Eq. (6) possesses the same ultraviolet divergence. It may therefore be eliminated by subtracting the  $\mu = 0 = T$  result. The subtraction can be accomplished by first recalling that for any function  $f(w)$  which is compatible with a physical system [40]:

$$2\pi iT \sum_{n=-\infty}^{\infty} f(i\omega_n + \mu) = \int_{u_\mu^*}^{u_0} dw f(w) - \int_{u_\mu^* + \eta}^{u_\mu + \eta} \frac{dw f(w)}{e^{(w-\mu)/T} + 1} - \int_{u_\mu^* - \eta}^{u_\mu - \eta} \frac{dw f(w)}{e^{-(w-\mu)/T} + 1}, \quad (7)$$

where we have omitted a  $T$ -independent term that is zero so long as  $\mu < \mu_c(T)$ , and  $u_\mu = i\Lambda + \mu$  with  $\Lambda \rightarrow \infty$ ,  $\eta \rightarrow 0$ . The first term on the right-hand-side of Eq. (7) is independent of  $(\mu, T)$  and responsible for the divergence we wish to eliminate. The physical piece of the dressed-quark pressure can thus be calculated as the difference between the two terms in the first line of Eq. (7), with  $f(w)$  computed via the functional expression in Eq. (6). Practically, one proceeds as follows: solve the gap equation at a given  $(\mu, T)$ -pair for a large number of Matsubara frequencies, characterised by  $n_m$ ; at each  $\mu$ , obtain smooth interpolations in “ $w$ ” for the three scalar functions obtained thereby, Eq. (2); evaluate  $P[S]$  with these inputs; and then compute the difference between the sum and integral, verifying that it is insensitive to the interpolation procedure and choice of  $n_m$ .

The pressure just described expresses our approximation for the dressed-quark contribution to the QCD EoS. In general, the pressure is weakly sensitive to  $T$  except in the neighbourhood of a phase transition. We denote the location of the maximum in the entropy density  $s(T) = \partial P[S]/\partial T$  by  $T_M$ . In connection with the chiral symmetry restoring phase transition at  $\hat{m} = 0$ ,  $T_M$  marks the critical temperature: the transition is second-order if  $s(T_M) < \infty$  and first order otherwise. In connection with a crossover at  $\hat{m} \neq 0$ ,  $s(T_M) < \infty$  and  $T_M$  is an associated pseudocritical temperature.

*3:Phase diagram and thermodynamics.*—We employ QCD's DSEs because they possess the capacity to study confinement and DCSB simultaneously in the continuum [41]. Within this framework the  $(\mu \neq 0, T \neq 0)$  EoS has only been computed using a very simple description of QCD's gauge sector [42]. Owing to the importance of the EoS in developing a complete picture of the Standard Model, it is imperative to do better.

Using our expression for the physical pressure, in Fig. 1 we depict the computed  $\mu = 0$  “trace anomaly,” *viz.*  $\mathcal{I} = \varepsilon - 3P$ , where the energy density  $\varepsilon = -P + Ts$ . Notably,  $\mathcal{I} \equiv 0$  for a noninteracting ultrarelativistic gas and hence  $\mathcal{I}$  is a measure of the interaction energy stored in the system. In this figure, the temperature is expressed in units of  $T_M = 0.14 \text{ GeV}$ .

Each computation in Fig. 1 is normalised by the appropriate form of  $P_{\text{SB}}$ : represented in this way, there is semi-

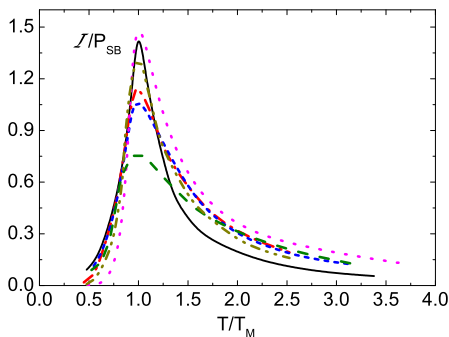


FIG. 1: Trace anomaly (normalised,  $\mu = 0$ ):  $\mathcal{I}/P_{\text{SB}}$ .  $P_{\text{SB}}$  is the pressure of a noninteracting ultrarelativistic gas containing the number of gluons and quarks appropriate to the calculation. Solid (black) curve – dressed-quark contribution, computed via Eq. (7). For comparison, lQCD results obtained using various discretisation schemes. Complete pressure: dot-dashed (red) and dot-dot-dashed (brown) curves [43]; short-dashed (blue) [44]; and long-dashed (green) [45]. Gluon-only contribution: dotted (pink) curve [46].

quantitative agreement between all results. One notes, however, that although the lQCD results in Refs. [43, 45] are both reported to describe the pressure of 2+1-flavour QCD, their results are not identical. Our prediction describes the quark-only contribution to  $\mathcal{I}$ . It matches the lQCD results in shape and order of magnitude. These observations indicate both that the gluon and quark contributions to the total interaction energy behave similarly and that they are commensurate in size when measured against their respective contributions to the pressure.

The “speed of sound” in the system is obtained from  $c_s^2 = \partial P / \partial \varepsilon$ . It is a crucial factor in determining the flow of material in the system, *i.e.* its transport properties. As evident in Fig. 2, our prediction for the sound velocity in the dressed-quark subcomponent is very similar to results obtained in lQCD for the velocity in the complete system.

A feature which distinguishes our framework from lQCD is its ability to treat  $\mu > 0$  without further approximation. Therefore, in Fig. 3 we display computed results for the dressed-quark pressure and trace anomaly at a range of values of  $\mu > 0$ . Plainly, whilst increasing  $\mu$  produces an increase in the pressure at all values of temperature, it only materially increases the interaction energy on  $T < T_M$ . Similar behaviour is seen in lQCD estimates for the  $\mu$ -dependence of these quantities, obtained using various extrapolation schemes [45, 47–49]. In detail,  $P$  is a monotonic function of  $T$  for small  $\mu$ , and  $P$  and  $\mathcal{I}$  are smooth; but qualitative changes occur at  $\mu = \mu_p = 0.106$  GeV: a peak appears in  $P$  and that in  $\mathcal{I}$  becomes sharper. Both functions remain smooth, however, until  $\mu = 0.111$  GeV, whereat the first derivative of each diverges at  $T = 0.128$  GeV, signalling that the transition has become first-order. This effect locates the critical endpoint (CEP) for the chiral symmetry restor-

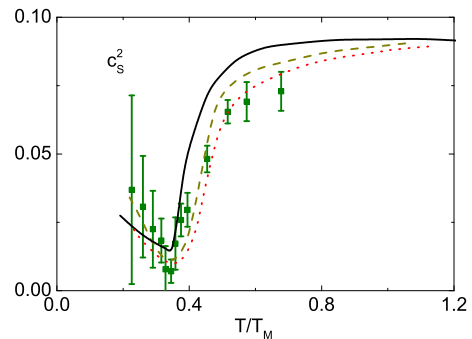


FIG. 2: Temperature dependence of  $c_s^2$ , where  $c_s$  is the sound velocity in the system. Solid (black) curve – our result, computed from the dressed-quark pressure; dashed (cyan) and dotted (red) curves – lQCD results from Ref. [43]; and points (green) – lQCD results from Ref. [45].

ing transition at  $(\mu_E^\chi = 0.111, T_E^\chi = 0.128)$  GeV. The behaviour of both  $P$  and  $\mathcal{I}$  on  $\mu/T \simeq 0$  is consistent with hard thermal loop perturbation theory [36].

This is an opportune point to draw the diagrams associated with QCD’s phase transitions as determined from the dressed-quark pressure. The restoration of chiral symmetry is straightforward. It may be explored by charting the  $(\mu, T)$ -dependence of the chiral condensate [50–52]; but we prefer to use a method based on the chiral susceptibility,  $\chi(\mu, T)$ , explained in Ref. [33].

Before discussing deconfinement, on the other hand, one must first have a definition of colour confinement; and we consider confinement as a violation of reflection positivity by coloured Schwinger functions. This position associates confinement with dynamically-driven changes in the analytic structure of QCD’s propagators and vertices [53–58]. Those changes occur because both gluons and quarks acquire running mass distributions, which are large at infrared momenta. The generation of these masses leads to the emergence of a length-scale  $\zeta \approx 0.5$  fm, whose existence and magnitude is evident in all existing continuum and lQCD studies of dressed-gluons and -quarks and which characterises the material change in their analytic structure (e.g. Refs. [7, 38, 59, 60]). From this perspective, deconfinement occurs when  $\zeta \rightarrow 0$  and reflection positivity is thus recovered. This criterion has been used effectively in dense-hot QCD (e.g. Refs. [27, 28, 34, 42, 61–63]; and we employ it herein, following a local implementation elucidated in Refs. [10, 64, 65].

We display the phase diagram computed from the dressed-quark pressure in Fig. 4. The solid curve describes the locus of zero pressure: the Nambu phase is energetically favoured for those values of  $(\mu, T)$  that lie within the domain bounded by the axes and this curve:

$$T_c^P(z = \mu/T_{c0}^P) = T_{c0}^P \frac{1 + 0.52z^2 - 0.058z^4}{1 + 0.91z^2}. \quad (8)$$

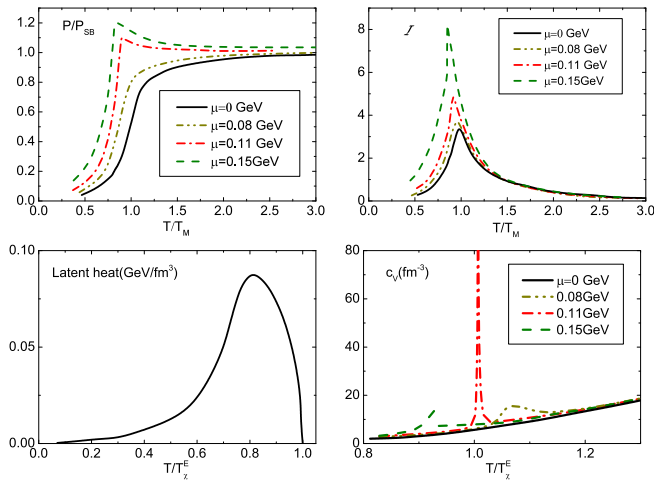


FIG. 3: *Upper panels*: Temperature dependence of the dressed-quark pressure (*left*) and trace anomaly (*right*) at several chemical potentials. *Lower left panel*: latent heat of the chiral symmetry restoring transition. *Lower right panel*: heat capacity of the system's dressed-quark subcomponent.

The  $\mu = 0$  pseudo-critical temperature associated with the chiral phase transition is  $T_{c0}^P = 0.15$  GeV, which may be compared with a recent IQCD estimate of the critical temperature for chiral symmetry restoration in QCD with two light flavours [66]:  $T_c = 0.15 \pm 0.01$  GeV.

With  $(\mu, T)$  increasing from the origin, the dot-dashed curve in Fig. 4 bounds the domain within which the Nambu-phase chiral susceptibility is positive. The dotted curve, on the other hand, marks the line whereat the Wigner-phase chiral susceptibility switches from negative to positive. These curves coincide with the zero-pressure locus, Eq. (8), up to the chiral transition's CEP:  $\text{CEP}_\chi = (\mu_E^\chi = 0.111, T_E^\chi = 0.128)$  GeV, which confirms the result obtained in connection with Fig. 3, top panels; and the computed ratio  $\mu_E^\chi/T_E^\chi = 0.87$  is commensurate with those in Refs. [33, 67–69]. The chiral crossover becomes a first-order transition at  $\text{CEP}_\chi$ : the Nambu and Wigner phases coexist, with the Nambu phase dominant below the zero-pressure locus and the Wigner phase dominant on the other side of this boundary.

The phase boundary for the deconfinement transition is marked by the dashed curve. This is a second-order transition until  $\text{CEP}_\zeta = (\mu_E^\zeta = 0.185, T_E^\zeta = 0.106)$  GeV,  $\mu_E^\zeta/T_E^\zeta = 1.75$ . In Wigner phase-domains one has neither confinement nor DCSB at any values of  $(\mu, T)$ . In the chiral limit the solid and dashed curves coincide and  $\text{CEP}_\chi = \text{CEP}_\zeta$ , *i.e.* chiral symmetry restoration and deconfinement are coincident. The dislocation at  $\hat{m} \neq 0$ , however, entails the existence of a small domain within which dressed-quarks are deconfined but chiral symmetry is broken. This is the set  $\{\mu, T\}$  enclosed within the dot-dashed and dashed curves. Pockets of Nambu phase material in this subset of the phase coexistence region possess that character. In the domain of  $(\mu, T)$  enclosed

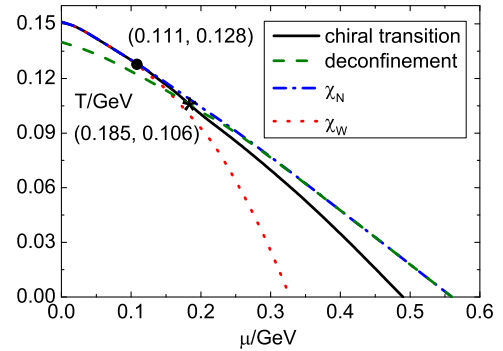


FIG. 4: Deconfinement and chiral symmetry restoration phase boundaries, computed via pressure in Eq. (7). Curves: solid (black) – chiral transition, with DCSB favoured below the curve; dashed (green) – deconfinement transition, with dressed-quarks confined below the curve; dot-dashed (blue) – Nambu phase chiral susceptibility,  $\chi_N$ : positive below the curve and zero above; dotted (red) – Wigner phase chiral susceptibility,  $\chi_W$ : positive *above* the curve and negative below. CEPs: chiral – filled circle; and deconfinement – asterisk.

between the axes and the dashed and dotted curves, the system is in a pure phase with confinement and DCSB, whereas chiral symmetry is restored and quarks are deconfined in the domain above the dot-dashed curve.

We are now in a position to compute the heat-capacity density of the system and the latent-heat density of transition:  $c_V = \partial \varepsilon / \partial T$ ,  $L = T \Delta s = \Delta \varepsilon - \mu \Delta \rho$ , respectively,  $\rho(T) = \partial P / \partial \mu$  is the quark number density and  $\Delta_F$  is the difference between the quantity  $F$  in the two distinct phases, which are here the Nambu (chirally asymmetric) and Wigner (chiral symmetry restored) phases. In the lower-left panel of Fig. 3 we depict the latent heat, computed along the phase boundary, which is the trajectory in Eq. (8). Naturally,  $L = 0$  for  $T \geq T_E^\chi$  because the transition is then second order. Otherwise our prediction is qualitatively consistent in shape with what may be inferred from existing IQCD simulations [45].

The lower-right panel of Fig. 3 depicts our prediction for the heat capacity: it diverges as  $(\mu, T) \rightarrow \text{CEP}_\chi$ . Actually, in the neighbourhood of the CEP one may write [70]:  $c_V \propto |g - g_E^\chi|^{-\epsilon}$ , where  $g = \mu, T$ ; and the quark number susceptibility  $\chi = \partial \rho / \partial \mu$  behaves in the same fashion. Analysing our results, we find  $\epsilon = 0.67 \pm 0.02$  in both cases. These are the critical exponents of a mean-field transition, which is the nature of RL truncation.

*4: Summary.* — We introduced a practical, numerically stable procedure for computing the  $(\mu, T)$ -dependent dressed-quark pressure in continuum QCD, which we illustrated using a gap equation whose solutions are key pieces in a widely used and successful description of the properties of ground-state hadrons in-vacuum. Without further approximation, the associated richly-structured phase diagram in the  $(\mu, T)$ -plane was computed. We

drew the transition lines for deconfinement and chiral symmetry restoration, and confirmed that these transition are identical in the chiral limit. Likewise, we calculated the speed of sound in the system and provided the  $(\mu, T)$ -dependence of the trace anomaly, latent-heat and heat-capacity densities. In cases where comparisons are possible, our predictions are consistent with results from lattice QCD. Notably, predictions obtained from the dressed-quark pressure are qualitatively and semi-quantitatively equivalent to those computed using the complete pressure, which suggests that the dressed-quark pressure alone can be used as a practical guide to QCD's thermal properties. No material improvement over our results can be envisaged in a continuum analysis before a symmetry-preserving kernel including long range correlations is derived for the gap equation. Our method for computing the pressure will also be applicable then.

*Acknowledgments.*— Work supported by: National Natural Science Foundation of China under Contract Nos. 11435001 and 11175004; the National Key Basic Research Program of China under Contract Nos. G2013CB834400 and 2015CB956900; the Office of the Director at Argonne National Laboratory through the Named Postdoctoral Fellowship Program; and the U.S. Department of Energy, Office of Science, Office of Nuclear Physics, under contract no. DE-AC02-06CH11357.

---

\* Corresponding author: yxliu@pku.edu.cn

† Corresponding author: cdroberts@anl.gov

- [1] J. C. Collins and M. J. Perry, Phys. Rev. Lett. **34**, 1353 (1975).
- [2] G. Baym, Nucl. Phys. A **698**, xxiii (2002).
- [3] M. Gyulassy and L. McLerran, Nucl. Phys. A **750**, 30 (2005).
- [4] P. Braun-Munzinger and J. Wambach, Rev. Mod. Phys. **81**, 1031 (2009).
- [5] K. Fukushima and T. Hatsuda, Rept. Prog. Phys. **74**, 014001 (2011).
- [6] S. J. Freedman *et al.*, Nuclear Physics: Exploring the Heart of Matter (National Academies Press, Washington D.C., 2012).
- [7] M. Bhagwat, M. Pichowsky, C. Roberts and P. Tandy, Phys. Rev. C **68**, 015203 (2003).
- [8] P. O. Bowman *et al.*, Phys. Rev. D **71**, 054507 (2005).
- [9] M. S. Bhagwat and P. C. Tandy, AIP Conf. Proc. **842**, 225 (2006).
- [10] C. D. Roberts, Prog. Part. Nucl. Phys. **61**, 50 (2008).
- [11] J. M. Cornwall, Phys. Rev. D **26**, 1453 (1982).
- [12] A. C. Aguilar and J. Papavassiliou, JHEP **0612**, 012 (2006).
- [13] P. Boucaud *et al.*, Few Body Syst. **53**, 387 (2012).
- [14] A. Ayala, A. Bashir, D. Binosi, M. Cristoforetti and J. Rodriguez-Quintero, Phys. Rev. D **86**, 074512 (2012).
- [15] D. Binosi, L. Chang, J. Papavassiliou and C. D. Roberts, Phys. Lett. B **742**, 183 (2015).
- [16] H. Politzer, Proc. Nat. Acad. Sci. **102**, 7789 (2005).
- [17] F. Wilczek, Proc. Nat. Acad. Sci. **102**, 8403 (2005).
- [18] D. Gross, Proc. Nat. Acad. Sci. **102**, 9099 (2005).
- [19] D. H. Rischke, Prog. Part. Nucl. Phys. **52**, 197 (2004).
- [20] P. Braun-Munzinger, B. Friman and J. Stachel, Nucl. Phys. A **931**, pp.1 (2014).
- [21] O. Philipsen, Prog. Part. Nucl. Phys. **70**, 55 (2013).
- [22] C. D. Roberts and S. M. Schmidt, Prog. Part. Nucl. Phys. **45**, S1 (2000).
- [23] P. Maris and C. D. Roberts, Int. J. Mod. Phys. E **12**, 297 (2003).
- [24] L. Chang, C. D. Roberts and P. C. Tandy, Chin. J. Phys. **49**, 955 (2011).
- [25] A. Bashir *et al.*, Commun. Theor. Phys. **58**, 79 (2012).
- [26] I. C. Cloët and C. D. Roberts, Prog. Part. Nucl. Phys. **77**, 1 (2014).
- [27] A. Bender, D. Blaschke, Y. Kalinovsky and C. D. Roberts, Phys. Rev. Lett. **77**, 3724 (1996).
- [28] A. Bender, G. I. Poulis, C. D. Roberts, S. M. Schmidt and A. W. Thomas, Phys. Lett. B **431**, 263 (1998).
- [29] P. Maris, C. D. Roberts, S. M. Schmidt and P. C. Tandy, Phys. Rev. C **63**, 025202 (2001).
- [30] H. J. Munczek, Phys. Rev. D **52**, 4736 (1995).
- [31] A. Bender, C. D. Roberts and L. von Smekal, Phys. Lett. B **380**, 7 (1996).
- [32] A. Höll, P. Maris and C. D. Roberts, Phys. Rev. C **59**, 1751 (1999).
- [33] S.-X. Qin, L. Chang, H. Chen, Y.-X. Liu and C. D. Roberts, Phys. Rev. Lett. **106**, 172301 (2011).
- [34] F. Gao, S.-X. Qin, Y.-X. Liu, C. D. Roberts and S. M. Schmidt, Phys. Rev. D **89**, 076009 (2014).
- [35] C. S. Fischer, J. Luecker and C. A. Welzbacher, Phys. Rev. D **90**, 034022 (2014).
- [36] N. Haque, M. G. Mustafa and M. Strickland, Phys. Rev. D **87**, 105007 (2013).
- [37] S.-X. Qin, L. Chang, Y.-X. Liu, C. D. Roberts and D. J. Wilson, Phys. Rev. C **84**, 042202(R) (2011).
- [38] F. Karsch and M. Kitazawa, Phys. Rev. D **80**, 056001 (2009).
- [39] R. W. Haymaker, Riv. Nuovo Cim. **14**, 1 (1991).
- [40] J. I. Kapusta, Finite-temperature field theory (Cambridge University Press, Cambridge UK, 1989).
- [41] L. McLerran and R. D. Pisarski, Nucl. Phys. A **796**, 83 (2007).
- [42] D. Blaschke, C. D. Roberts and S. M. Schmidt, Phys. Lett. B **425**, 232 (1998).
- [43] A. Bazavov *et al.*, Phys. Rev. D **80**, 014504 (2009).
- [44] P. Huovinen and P. Petreczky, Nucl. Phys. A **837**, 26 (2010).
- [45] S. Borsanyi *et al.*, JHEP **1208**, 053 (2012).
- [46] G. Boyd *et al.*, Nucl. Phys. B **469**, 419 (1996).
- [47] Z. Fodor, S. D. Katz and K. K. Szabó, Phys. Lett. B **568**, 73 (2003).
- [48] C. Allton *et al.*, Phys. Rev. D **68**, 014507 (2003).
- [49] C. DeTar *et al.*, Phys. Rev. D **81**, 114504 (2010).
- [50] S. J. Brodsky, C. D. Roberts, R. Shrock and P. C. Tandy, Phys. Rev. C **82**, 022201(R) (2010).
- [51] L. Chang, C. D. Roberts and P. C. Tandy, Phys. Rev. C **85**, 012201(R) (2012).
- [52] S. J. Brodsky, C. D. Roberts, R. Shrock and P. C. Tandy, Phys. Rev. C **85**, 065202 (2012).
- [53] V. N. Gribov, Eur. Phys. J. C **10**, 91 (1999).
- [54] H. J. Munczek and A. M. Nemirovsky, Phys. Rev. D **28**, 181 (1983).
- [55] M. Stingl, Phys. Rev. D **29**, 2105 (1984).
- [56] R. T. Cahill, Austral. J. Phys. **42**, 171 (1989).

- [57] C. D. Roberts, A. G. Williams and G. Krein, *Int. J. Mod. Phys. A* **7**, 5607 (1992).
- [58] F. T. Hawes, C. D. Roberts and A. G. Williams, *Phys. Rev. D* **49**, 4683 (1994).
- [59] P. O. Bowman *et al.*, *Phys. Rev. D* **76**, 094505 (2007).
- [60] S. Strauss, C. S. Fischer and C. Kellermann, *Phys. Rev. Lett.* **109**, 252001 (2012).
- [61] J. A. Mueller, C. S. Fischer and D. Nickel, *Eur. Phys. J. C* **70**, 1037 (2010).
- [62] S.-X. Qin, L. Chang, Y.-X. Liu and C. D. Roberts, *Phys. Rev. D* **84**, 014017 (2011).
- [63] S.-X. Qin and D. H. Rischke, *Phys. Rev. D* **88**, 056007 (2013).
- [64] A. Bashir, A. Raya, I. C. Cloët and C. D. Roberts, *Phys. Rev. C* **78**, 055201 (2008).
- [65] A. Bashir, A. Raya, S. Sánchez-Madrigal and C. D. Roberts, *Few Body Syst.* **46**, 229 (2009).
- [66] A. Bazavov *et al.*, *Phys. Rev. D* **85**, 054503 (2012).
- [67] Z. Fodor and S. D. Katz, *JHEP* **0404**, 050 (2004).
- [68] C. Schmidt, *J. Phys. G* **35**, 104093 (2008).
- [69] C. S. Fischer and J. Luecker, *Phys. Lett. B* **718**, 1036 (2013).
- [70] Y. Hatta and T. Ikeda, *Phys.Rev.* **D67**, 014028 (2003).